Detection of Marine Debris by Surveillance of Coral Bleaching and Temperature Anomaly using Satellite Imagery

Shivaani Suseendran[1*], Charanya Manivannan[1], Jovina Virgin[1] and Dr. Vani K.[1]

[1]Department of Information Science and Technology, College of Engineering Guindy, Chennai, India

*shivaanis32@gmail.com

Abstract: *Effects like bleaching of corals and anomalies in temperature can directly or indirectly be connected with the presence of debris. In this study, methods of finding debris, if bleaching or sea surface temperature anomaly is found are implemented. The dependent factors affecting bleaching were found by analyzing the p-scores from logistic/ordinary least squares regression models and correlation using the global corals' distribution datasets. Ground truth was combined with spectral indices such as the Normalized Difference Vegetation Index, Normalized Difference Turbidity Index, Benthic Cover Index, Algae Index, Normalized Salinity index, Normalized Pigment Index, Sedimentation Stress Index, Pollutant Concentration Index, Thermal Stress Index, and Coral Health Index calculated based on factors got. The Naive Bayes model trained for classification achieved an accuracy of 0.95. Similarly, sea surface temperature data for the years 2019-2023 were downloaded and a Long Short-Term Memory model was trained whose R-squared score was 0.98. The temperature for the future date is forecasted and compared with the actual temperature on that date. If the difference was above 0.005, it was flagged to have an anomaly, and this threshold was set by observing the extremities of the temperature range. If any of these two are found, the image is passed to the debris detection model after cloud and land masking. This XGBoost model (accuracy of 0.99) is trained with a readily available labeled dataset consisting of band values from Band-0 to Band-12 and indices such as the Floating Debris Index, Normalized Difference Water Index, Automated Water Extraction Index, Anthocyanin Reflectance Index, Red-Edge Position Index, Normalized Burn Ratio, Oil Spill Index and so on. The outcomes were validated with existing data.*

Keywords: Debris detection, Satellite image processing, Spectral indices, Surveillance of coral bleaching for debris, Surveillance of temperature anomaly for debris.

Introduction

Pollution in the oceans is increasing because there are no proper monitoring mechanisms for it. Marine life and environmental risks are bad when too much debris is left in seas, that's why it is really important to identify it and remove it from there. This presence of debris can lead to many effects like bleaching of corals, anomalies in temperatures, etc. Automated strategies beef up the efficiency of this activity, especially in hard-to-reach zones. Use of Remote sensing will help with the implementation of these. It helps in detecting objects, including debris from satellite images, by analyzing its frequency and wavelength values in

the electromagnetic spectrum. In this research, advanced ways to find debris are found by investigating coral bleaching and sea surface temperature anomalies by combining statistical models and spectral indices into a machine learning system which can serve as a good tool for an appropriate yet efficient surveillance of the surroundings. With the help of Machine Learning (ML) and Artificial Intelligence (AI) technologies, these functionalities are implemented.

Literature Review

As the population and the garbage in water rise, the need for monitoring them also increases. The accumulation of garbage in rivers, lakes, and oceans, presents significant challenges for environmental health and marine ecosystems. The effect on the health of corals along with other properties like bleaching are also necessary to be studied. Their effect on the temperature anomalies can also be assessed. The effect of bleaching of corals was first provided by using Depth Invariant Indices (DII) and spectral simulation, by Ove et al (2017). The steps include image preprocessing, atmospheric correction, geo-registration, and masking. Radiometric normalization is compared, scene to scene, with the use of Pseudo-Invariant Features and DII. Data used in this study include multi-temporal Sentinel-2 images, where change analysis is done using two images taken at different dates. In this study, there is spectral simulation using an Semi-Analytical (SA) model and a processed image classifier with the Support Vector Machine (SVM) algorithm. The Accuracy of the bleached coral maps obtained through the PIFs and DII approaches are found to be 88.9% and 57.1%, respectively.

Another work created a supervised image classification model for the detection of coral bleaching at coastal areas of Iriomote and Ishigaki Islands in Japan by making use of bi-temporal Sentinel-2 satellite image data. This was put forth by Narciso G. A. M. et al (2023). In this regard, the Random Forest algorithm was applied in attaining high accuracy in the classification of events such as bleaching, seagrass/macroalgal growth, cloud covers, and wave foams. The overall accuracies obtained were 0.97 while the kappa statistic values were 0.94. The validation of the study used insitu data which showed a percentage agreement of 78%. This study has pointed out changes and temporal patterns in benthic habitats.

Similarly, techniques for the identification of temperature anomalies are also proposed. In the work of Liu et al (2021), a Sentinel-2 Multi-Spectral Instrument (MSI) image was used to develop a Thermal Anomaly Index (TAI) that has the capability of detecting High

Temperature Anomalies (HTA) as a result of phenomena like fires, industry activities, and volcanic activities. The equation for TAI has been derived from spectral characteristics in various bands basically to enhance HTAs that takes into far- Short Wave Infrared (SWIR), near-SWIR, and Near Infrared (NIR) bands $(\rho far\text{-}SWIR - \rho near\text{-}SWIR)/\rho NIR \geq 0.45$ and $(\rho far\text{-}SWIR - \rho near\text{-}SWIR) \geq \rho near\text{-}SWIR - \rho NIR)$. Sentinel-2 MSI images, AVIRIS data, and Landsat-family satellite images were utilized in this study for the identification of several HTAs such as wildfires, industrial heat sources, and volcanic thermal anomalies. This approach showed high accuracy rates: 99.5% of HTA pixels have TAI values ≥ 0.45 while 78.1% of the HTA pixels showed TAI values ≥ 1.

Marine litter needs to be detected and classified to ensure the protection of the environment and safety at sea. The dataset used for this study is obtained by Achille Carlo Ciappa et al (2022) in the North Adriatic in August 2020 of six scenes from the Sentinel-2 mission. Floating patches were found in band 8 (NIR) because they reflect more in this range. To distinguish marine litter mixed with vegetal materials and to detect floating materials, anomalies in the Red Edge bands were analyzed with thresholds set to classify pixels as vegetal if >0.50, intermediate if in 0.25-0.50, and if <0.25, then both mixed marine litter and vegetal. They are said to be unclassified if their ratio is less than or equal to 0.01**.** 16% of floating materials were classified as such. The study classified pixels based on spectral differences, particularly in the Red Edge bands, to discriminate between different types of floating materials, including marine litter.

Another type of debris classification into 7 classes was provided by Miguel M. Duarte et al (2023). They were water, plastic, seaweed, driftwood, sea snot, pumice and sea foam. A Wasserstein Generative Adversarial Network (WGAN) was used to expand the dataset values. The data was from published works and manual satellite image interpretation. In situ data from vessels and diving expeditions were used to manually detect plastic litter by comparing spectral responses with literature values for Sentinel-2's multispectral instrument. Permutation importance matrices were created to analyze the important features affecting the accuracy. Each of the attribute gets assigned an importance value. Reflectance indices for each object were calculated, achieving over 85% accuracy.

An extension of these to identify waste is being done in this paper. Once impacts like coral bleaching/temperature anomaly are identified, the image is fed to a model to detect the presence of debris and if present then it may be a reason for the impact. A rough computation

of the area is also provided. Various models are analyzed and compared. The approaches followed are explained in detail in the upcoming sections of this paper. The results were also validated with actual data from the public domain.

Methodology

The processes are described in detail along with the methodologies and data below.

Data Collection

Locations of bleached and unbleached corals are obtained from the ArcGIS website. The sentinel-2 images of these corals are downloaded from the Google Earth Engine (GEE) after cloud masking. The global corals dataset is downloaded from the public domain. Similarly, sea surface temperature data for five years 2019-2023 is downloaded from the National Centers for Environmental Information (NCEI) websites in the form of .nc files. For debris detection a dataset with 60,807 values (24 indices) is downloaded from GitHub.

Data Preprocessing and Dataset Creation

From the global corals' dataset, the factors dependent on the bleaching of corals like temperature and salinity are found using correlation, Ordinary Linear squares regression (OLS), and Logistic Regression. Using z and Wald's tests, the p values and f values are found. If the p values are less than 0.05, it implies that the null hypothesis which says that one factor is independent on the outcome is rejected. Similarly, a positive coefficient of an attribute obtained during regression means that it significantly affects the target variable. These coefficients and p scores are observed. So based on these, factors such as temperature, salinity, and silt/sulfide (sediments) are obtained. The spectral Indices pertaining to these are calculated after cloud and land masking of the sentinel images of corals. The dataset made has 2611455 rows and 23 columns of bands and indices values. Land masking is done to highlight the water bodies. The calculated indices along with the ground truth are made into a data frame.

The temperatures are extracted from the .nc files and null values are removed and the date of each file along with its temperature data is stored as a data frame resulting in about 1 crore rows. This broad dataset has information regarding dates and temperatures, which will subsequently be made into a visualization to demonstrate the trends and patterns. It is possible to get insight into seasonal variations, long-term trends of temperature, and spatial differences from different visualization methods such as time series plots, heat maps, and

histograms. All these procedures, other than being helpful to learn about temperature dynamics, also give support to further analyses and predictive modeling in such comprehensive environmental studies.

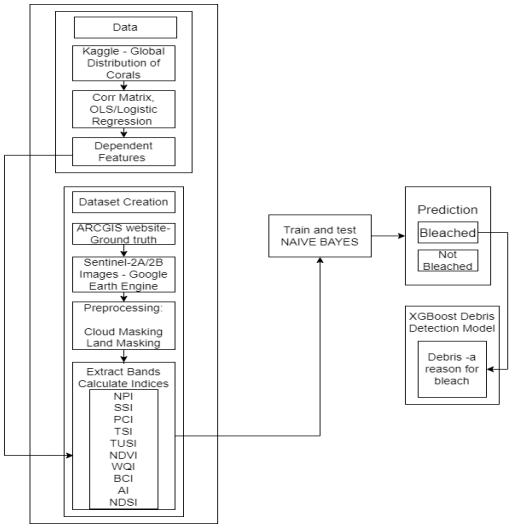

Figure 1: Architecture for coral bleaching

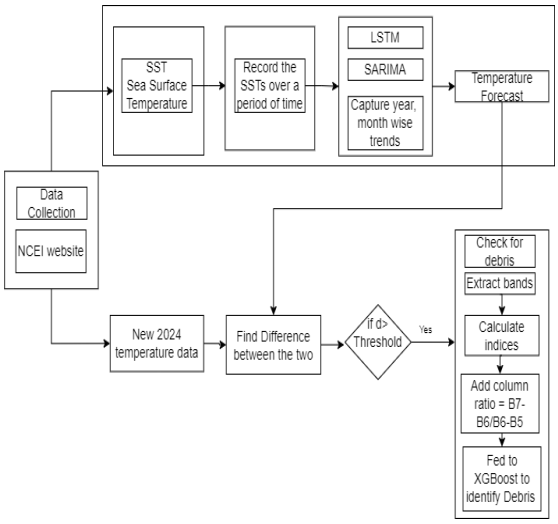

Figure 2: Architecture for temperature anomaly

Both the processes are displayed in detail by the architectures in Figures 1 and 2. The sections to follow will take the user through a step-by-step, detailed, and full walk-through of how each stage in the model's development was carried out. This means that the whole process, starting from the initial and final phase of design and moving through to final implementation and evaluation, is covered in detail.

Method and Model Development

Coral Bleaching

First of all, the sentinel images are cloud, cirrus, and land-masked. This is done to remove these objects and highlight the water body alone. 1<<10 is Cloud mask and 1<<11 is Cirrus mask. Normalized Difference Water Index (NDWI) is calculated and compared with a threshold to visualize the water body highlighting. The NDWI is calculated by, NDWI $= \frac{\square 4 - \square 8}{\square 4 + \square 8}$. The threshold that is set is based on the value at which the water bodies can be observed clearly (bright white color). The rest of the land is made black. This is done by visualizing the image. The ground truth is obtained from the Arcgis website which provides locations of - healthy, mediumly bleached, and most bleached corals. Secondly, the regressions are performed and their coefficients and p values are noted down. In general, a p-value measures the probability of observing an effect at least as extreme as the one in the sample data, assuming that the null hypothesis is true. The null hypothesis typically posits

that there is no effect or no relationship (e.g., no linear relationship between the independent and dependent variables in the context of regression). If p-value < 0.05, then the null hypothesis is rejected, meaning the outcome is dependent on that particular factor. Other spectral indices calculated are given in Table 1.

Table 1: Spectral Indices and their Formula for coral bleaching

Indices	Formula
Normalized Difference Moisture Index (NDMI)	$\frac{□8 - □11}{□8 + □11}$
Normalized Difference Turbidity Index (NDTI)	$\frac{□3 - □2}{□3 + □2}$
Normalized Difference Vegetation Index (NDVI)	$\frac{□8 - □4}{□8 + □4}$
Normalized Difference Salinity Index (NDSI)	$\frac{□□□□ + □□□□}{2}$
Normalized Pigment Index (NPI)	$\frac{□8 - □5}{□8 + □5}$
Sedimentation Stress Index (SSI)	$\frac{□4}{□3}$
Pollutant Concentration Index (PCI)	$\frac{□4 - □2}{□4 + □2}$
Thermal Stress Index (TSI)	$\frac{□12 - □11}{□12 + □11}$
Benthic Cover Index (BCI)	$\frac{□4}{□8}$
Algae Index (AI)	$\frac{□8 - □5}{□8 + □5}$
Coral Health Index (CHI)	$\frac{□8}{□4}$

Naive Bayes model is trained with these indices and ground truth (80% train and 20% test).

Temperature Anomaly: From the temperature dataset, a Long Short-Term Memory (LSTM) model is trained to capture the trends of the temperature on a daily and a monthly trend. A Seasonal Autoregressive Moving Average (SARIMA) model is also trained and its parameters (seasonal and non-seasonal) are fine-tuned. The objective of this is to forecast the sea surface temperature at a future date and compare it with the actual temperature on that particular day. This data was also obtained from the same NCEI site. The ranges of the temperature collected are observed. Its distribution was close to normal so the statistical methods like mean, median and $\pm 3\square$ are analyzed and the threshold is set to be 0.005 on observing the ranges. If Forecasted $_{temperature}$ - Actual $_{temperature}$ >0.005, then it is flagged as an anomaly. Hence it is passed on to the debris detection model as there is an anomaly found.

Table 2: Parameter fine tuning for time series and naive bayes

Model	Method	Parameters	Optimized performance at
SARIMA	Manual Grid Search	(p,q,d)(P,Q,D,S)	(2,1,2) (1,1,2,12)
LSTM	Manual Grid Search	Layers	Layers: LSTM(150) returning sequences to allow stacking LSTM(150), compresses these sequences into a single output vector Dense(150) Dense(1)
Gaussian naive bayes	Grid Search	var_smoothing : [1e-9, 1e-8, 1e-7, 1e-6, 1e-5]	Best at 1e-9

Debris Detection

The downloaded dataset has 60,807 values and is fed to XGBoost, Naive Bayes, Random Forest, Artificial Neural Networks (ANN), and K Nearest Neighbors (KNN) and performances are compared. the non-debris pixels are colored black and debris pixels are colored white. It had 7 classes and it could be classified via 7 as well. Parameters like maximum depth, learning rate, and n_esitimators are all fine-tuned using GridSearch CV for XGBoost and Random Forest. The K value for KNN was found using the cross-validation method. The bands extracted are normalized by raising to 10^{-4}. In addition to the indices given in Table 1, another column called ratio which is basically the difference between the Red Edge bands, which helps in discriminating vegetation, Ratio: $\frac{\square 7-\square 6}{\square 6-\square 5}$. First of all, the

values of the bands were read using the Python rasterio library for processing geospatial raster data. Then, the performances of each model were compared by several performance metrics in order to find out which approach gives the best predictive accuracy for the task at hand. The hyperparameter tuning performed is detailed in Table 3. Table 4 gives the list of indices for debris detection.

Table 3: Optimum parameter values for debris detection models

Model	Method	Parameters	Optimized values
XGBoost	Grid Search CV	learning rate: [0.01, 0.1, 0.3, 0.5, 0.7] Max depth: [3,6,9] n_estimators: [50, 100, 200 ,300]	learning rate-0.3, maximum tree depth-3, n_estimators-200.
Random Forest Classifier	Grid Search CV	n_estimators: [50, 100, 150, 200], max_depth: [None, 10, 20, 30], min_samples_split: [2, 5, 10], bootstrap: [True, False]	n_estimators: 100, max_depth: 10, min_samples_split: 2, bootstrap: True
KNN	Grid Search CV	n_neighbors: [range(1,21)], (with cv as 5)	K=1

Rough Area Computation/ Percentage of Waste: This is done by first extracting the spatial resolution from the image. The term Spatial Resolution means the size/dimension of the smallest feature that can be recognized by a satellite sensor or displayed in a satellite image and is usually presented in the form of a single value which is basically denoting the length of one side of a square. The number of garbage and non-garbage pixels are calculated from the detection. Pixel width and height are extracted from affine transformation for spatial resolution.

$$\text{Pixel}_{\text{Area}} = (\text{Spatial Res})^2,\ \text{Debris}_{\text{Area}} = \text{Pixels}_{\text{Debris}} \times \text{Pixel}_{\text{Area}}$$

$$\text{Density in terms of area} = \frac{\text{Debris}_{\text{Area}}}{\text{Debris}_{\text{Area}} + \text{Water}_{\text{Area}}}$$

Table 4: Spectral Indices and their Formula for debris detection

Index Name	Formula
Plastic Index (PI)	$\frac{□8}{□8+□4}$
Normalized Difference Water Index (NDWI)	$\frac{□3-□8}{□8+□3}$
Water Ratio Index (WRI)	$\frac{□3+□4}{□8+□12}$
Automated Water Extraction Index (AWEI)	4 x (B3 + B12) - (0.25 x B8 + 2.75 x B11)
Modified Normalization Difference Water Index (MNDWI)	$\frac{□3-□12}{□4+□12}$
Simple Ratio (SR)	$\frac{□8}{□4}$
Reversed Normalized Difference Vegetation Index (RNDVI)	$\frac{□4-□8}{□8+□4}$
Anthocyanin Reflectance Index (ARI)	$\frac{1}{□3}-\frac{1}{□5}$
Modified Anthocyanin Reflectance Index (MARI)	$\frac{1}{□3}-\frac{1}{□5}$x B7
Chlorophyll Red-Edge (CHL_RedEdge)	$\frac{□8}{□5}-1$
Red Edge Position Index (REPI)	$700+40\ x\ \frac{\frac{□4+□7}{2}-□5}{□6-□5}$
Enhanced Vegetation Index (EVI)	$2.5\ x\ \frac{□8-□4}{□8+6\times□4-7.5\times□2+1}$
Green Normalized Difference Vegetation Index (GNDVI)	$\frac{□8-□3}{□3+□8}$
Modified Chlorophyll Absorption in Reflectance Index (MCARI)	$(B5-B4)-0.2\ x\ (B5-B3)\ x\ \frac{□5}{□4}$
Moisture Index (MSI)	$\frac{□11}{□8}$

Normalized Difference Moisture Index (NDMI)	$\frac{□8 - □11}{□8 + □11}$
Normalized Burn Ratio (NBR)	$\frac{□8 - □12}{□8 + □12}$
Normalized Difference Snow Index (NDSI)	$\frac{□3 - □11}{□3 + □11}$
Soil Adjusted Vegetation Index (SAVI) (L=0.5)	$\frac{□8-□4}{□8+□4+0.5}$ x 1.5
Oil Spill Index (OSI)	$\frac{□3 + □4}{□2}$
Pan Normalized Difference Vegetation Index (PNDVI)	$\frac{□8 - (□2 + □3 + □4)}{□8 + □3 + □2 + □4}$
Normalized Difference Vegetation Index (NDVI)	$\frac{□8 - □4}{□8 + □4}$
Floating Debris Index (FDI)	B8 - (B6 + (B11 - B6)) x $\frac{833-665}{1610.4-665} \times 10$

Results and Discussion

As discussed above, the correlation of the features in the global distribution dataset is displayed in Figure 2. Corals are strongly correlated with the salinity of seas (0.832), and temperatures in January (0.503). From the Walds test, p scores are lesser than 0.05, meaning those features affect the health of corals. From the z test, the p score of salinity is less than 0.05, whereas the coefficients of salinity and temperature are also positive, meaning they may be significant. These three are taken as some of the significant factors and the spectral indices calculated based on this are displayed in Figure 3.

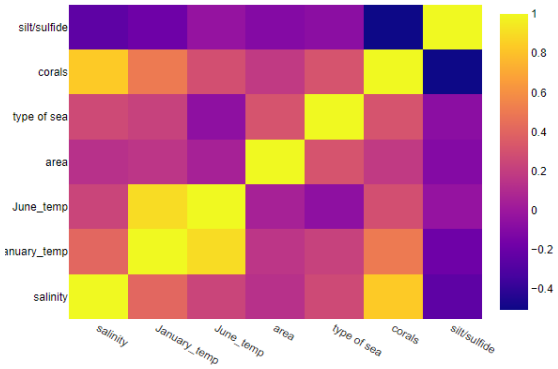

	Coef.	Std.Err.	z	P>|z|	[0.025	0.975]
silt/sulfide	-27.0779	169281.4761	-0.0002	0.9999	-331812.6743	331758.5185
salinity	0.0830	0.0397	2.0908	0.0365	0.0052	0.1608
June_temp	0.0060	0.0565	0.1059	0.9157	-0.1048	0.1168

(a)

```
Wald test results (corals = silt/sulfide): <F test: F=array([[1.3443859e+30]]), p=0.0, df_denom=46, df_num=1>
Wald test results (corals = June_temp): <F test: F=array([[1.20170405e+30]]), p=0.0, df_denom=46, df_num=1>
Wald test results (corals = January_temp): <F test: F=array([[1.10141386e+30]]), p=0.0, df_denom=46, df_num=1
>
Wald test results (corals = salinity): <F test: F=array([[1.09437043e+30]]), p=0.0, df_denom=46, df_num=1>
```

(b)

Figure 3: Correlation, p- values for factors affecting bleaching

The trained Naive Bayes model achieved the metrics shown in Table 5. Precision answers how frequently the predictions for the positive class are correct (true positives), and recall measures how well the model identifies all instances with positive classes in the dataset. The F1 score combines both precision and recall and is basically the harmonic mean of precision and recall.

Table 5: Metrics of Naive Bayes model

Precision	**Recall**	**F1-score**	**Accuracy**
0.93	0.96	0.95	0.95

Figure 4(a) illustrates the results of the corals present in Lakshadweep islands. The bleached part of the corals and the debris are colored and overlaid. Another region used is the corals from Handerson reefs with legends also displayed beside. All the debris pixels colored are colored separately and water pixels are colored separately. The next step is identifying if debris is present over the bleached area.

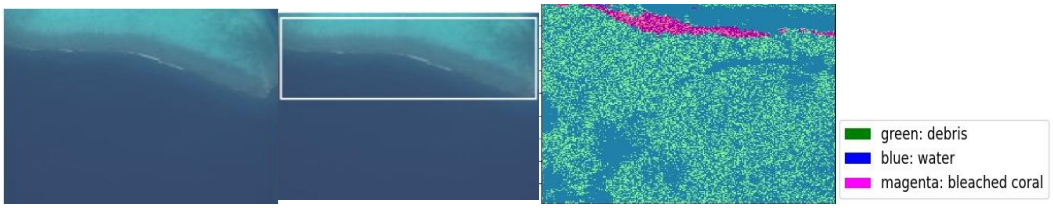

(a)

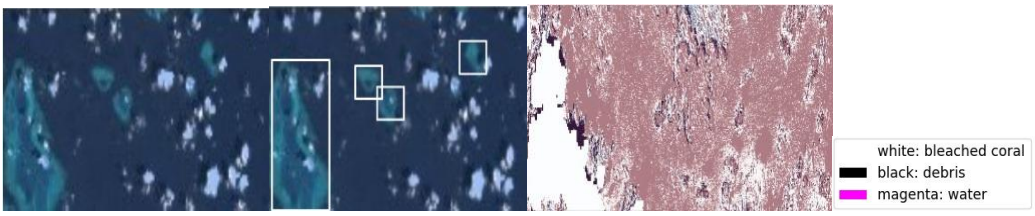

(b)

Figure 4: Debris across the coral-bleached areas (a is Lakshadweep and b is Handerson)

By detecting coral bleaching and identifying debris presence, it provides comprehensive insights that aid in pinpointing stress factors affecting reefs. So with this, extra attention can be specifically provided to these areas and cleanup processes can be done. The dataset for finding temperature anomalies is shown in Figure 5. The temperature for the next whole year is calculated. Based on the day entered, the corresponding value is obtained from the array. Various layers are permuted in the LSTM to find the one with the highest R^2. The (p,q,r)(P, Q, R, S) of SARIMA is also computed using different values of them and by analyzing the autocorrelation function as well. Since LSTM outperforms SARIMA, it is used as the final model.

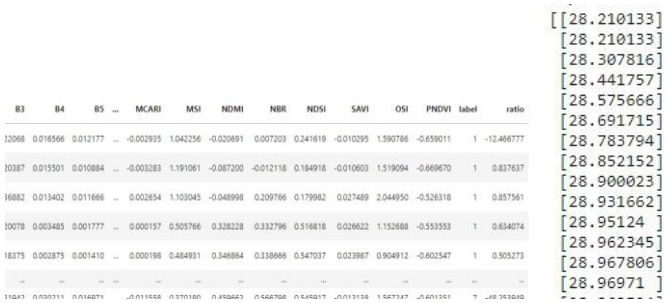

Figure 5: Dataset and the predicted temperatures for 2024

If the difference between the actual temperature and the predicted temperature exceeds the threshold, then there is an anomaly and so it is fed to the XGBoost model for debris detection. The non debris pixels are colored black and debris pixels are colored white. If a lot of debris is found, then it may be one of the reasons for the anomaly (global warming). The outputs are displayed along with the inputs on the UI. The predicted temperature array is of length 365 (one whole year data).

Table 6: Metrics of temperature forecasting models

MODEL	R^2	RMSE	MAE	MSE
LSTM	0.983	0.013	0.011	0.00017
SARIMA	0.73	0.117	0.09	0.130

The models are fine-tuned and evaluated as shown in Table 6. A measure of the proportion of variance is provided by R^2 score (R-squared). The Root Mean Square Error (RMSE) is the square root of the mean of the squared differences between the predicted and observed values, thereby giving greater weight to larger errors. The average of the absolute differences is given by Mean Absolute Error (MAE), which treats all errors equally. Mean Squared Error (MSE) averages squared differences, heavily penalizing larger errors and remaining in squared units. R^2 assesses model fit, while RMSE, MAE, and MSE measure prediction error, with RMSE and MSE being more sensitive to outliers than MAE.

```
Day:  2024-02-15
Forecasted Temperature:  28.969524
Actual Temperature:  28.991566
Difference:  0.022041704345703295
```

Figure 6: Output of anomaly found

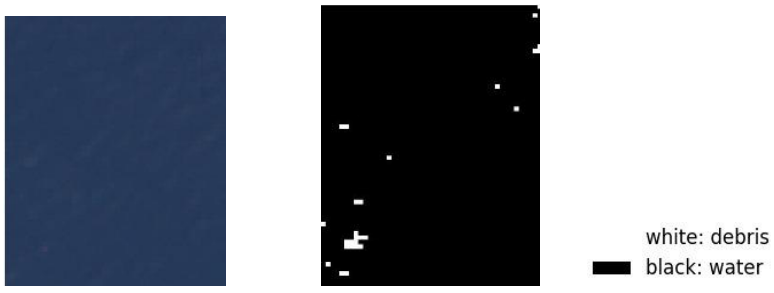

(a) (b) (c)

Figure 7: Presence of debris after anomaly detection

The details on date and temperatures are displayed in Figure 6. The white spots in Figure 7(b) indicate the debris present in Figure 7(a) and hence it may be a reason for the anomaly. The date provided as input is split and the temperature for that day is forecasted from the time series models. The predicted temperature for that date is compared with the actual temperature on that date. This is stored in the local system by extracting the information from

the .nc files. The names of the files are compared with the dates and matched. If it matches, then its temperature is differenced from the forecasted one for anomaly detection. Hence, the project investigates the utilization of temperature anomalies to detect the presence of debris within areas of interest, providing an additional layer of detection capability.

Table 7: Metrics of debris detection models

Model	Precision	Recall	F1-score	Accuracy
XGBoost	0.983	0.936	0.958	0.999
Naive Bayes	0.90	0.88	0.72	0.90
Random Forest	0.986	0.954	0.969	0.994
ANN	0.960	0.950	0.954	0.998
KNN	0.990	0.809	0.843	0.99

The performance metrics of all the models used are shown in Table 7. For all of these models, the parameters are fine-tuned. Above-mentioned functionalities—starting from image preprocessing to machine learning model prediction/forecasting—are combined in an interactive User Interface (UI) in a web-based interface using Flask, which provides an integrated platform for the management.

Conclusion and Recommendation

This approach will efficiently make use of coral bleached and temperature anomalies, thus improving debris detection. This integrated environmental monitoring allows the fine-scale and more accurate detection of debris, providing a better use of resources and better outcomes in marine debris management. The collected temperature data was trained using LSTM and SARIMA models and the monthly temperature patterns were captured and understood. A higher R^2 score of 0.98 was achieved by LSTM. The temperatures for 2024 were forecasted. If an anomaly was detected, the image was preprocessed for cloud and land

masking and checked for debris. Similarly, coral bleaching is monitored, and the affected areas are checked for debris. Using global coral distribution data, dependent features like salinity and temperature were analyzed with logistic regression and correlation, and indices related to these features were computed and combined with ground truth. Naive Bayes for bleaching prediction showed 0.95 accuracy. An accuracy of 0.99 was shown by the XGBoost debris detection model. It took into account 24 indices for classification. The findings bring valuable clues about the connection between environmental patterns and the health of the sea, helping to construct a dependable skeleton for any future endeavors concerning monitoring and minimizing risks in sea ecosystems. Hence, this study contributes to the effective usage of AI and ML in Remote Sensing. Future work will focus on refinement of the models and furthering analysis so that there is potential coverage for a wider range of marine environments and threats that can further aid the global conservation efforts of the world's oceans.

References

Achille Carlo Ciappa. (2022). Marine litter detection by Sentinel-2: A case study in the North Adriatic (summer 2020). *Remote Sensing, 14*(10), 2409. https://doi.org/10.3390/rs14102409

Duarte, M. M., & Azevedo, L. (2023). Automatic detection and identification of floating marine debris using multispectral satellite imagery. *IEEE Transactions on Geoscience and Remote Sensing, 61*, 1-15. https://doi.org/10.1109/TGRS.2023.328360

Hoegh-Guldberg, O., Skirving, W., Dove, S., & Poloczanska, E. S. (2017). Coral reef ecosystems under climate change and ocean acidification. *Frontiers in Marine Science, 4*. https://doi.org/10.3389/fmars.2017.00158

Liu, Y., Zhi, W., Xu, B., Xu, W., & Wu, W. (2021). Detecting high-temperature anomalies from Sentinel-2 MSI images. *ISPRS Journal of Photogrammetry and Remote Sensing, 177*, 174-193. https://doi.org/10.1016/j.isprsjprs.2021.05.008

Narciso, G. A. M., Tamondong, A. M., Blanco, A. C., Nakamura, T., & Nadaoka, K. (2023). Supervised image classification model for coral bleaching detection using a bi-temporal Sentinel-2 image stack. *The International Archives of the Photogrammetry, Remote Sensing and Spatial Information Sciences, XLVIII-4*. https://doi.org/10.5194/isprs-archives-XLVIII-4-W8-2023-395-2024